ACS APPLIED MATERIALS & INTERFACES

Letter

www.acsami.org

Formation of GaP/Si(100) Heterointerfaces in the Presence of Inherent Reactor Residuals

Oliver Supplie,*[,†,‡,§] Matthias M. May,[†,‡,§] Christian Höhn,[‡] Helena Stange,[‡] Antonio Müller,[†] Peter Kleinschmidt,[†] Sebastian Brückner,[†,‡] and Thomas Hannappel[†,‡]

[†]Institut für Physik, Technische Universität Ilmenau, 98693 Ilmenau, Germany

[‡]Institute for Solar Fuels, Helmholtz-Zentrum Berlin für Materialien und Energie, 14109 Berlin, Germany

[§]Institut für Physik, Humboldt-Universität zu Berlin, 12489 Berlin, Germany

ABSTRACT: Adequate silicon preparation is a prerequisite for defect-free III−V growth on Si. We transfer the silicon processing from clean to GaP containing metalorganic vapor phase epitaxy reactors, where we monitor the entire process in situ with reflection anisotropy spectroscopy and analyze the chemical composition of the surface with X-ray photoelectron spectroscopy. Beyond a certain submonolayer threshold value of (Ga,P) residuals found on the Si(100) surface, GaP grows with an inverted majority sublattice. Analogously to III−V growth on two-domain substrates, the coexistence of Si−Ga and Si−P interfacial bonds at terraces of the same type causes antiphase disorder in GaP epilayers.

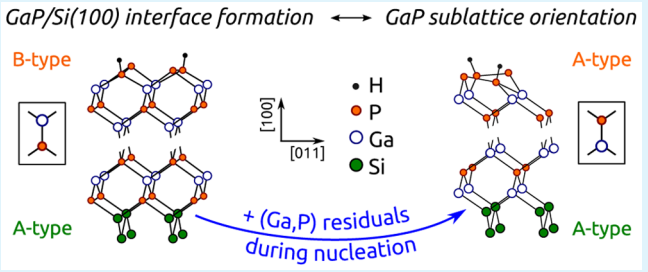

KEYWORDS: *heterointerfaces, III−V on silicon, optical in situ spectroscopy, photoelectron spectroscopy*

The integration of III−V semiconductors and silicon is highly desired in both microelectronics and photovoltaics. Adequate Si(100) surface preparation is decisive for the quality of subsequently grown GaP epilayers, which could serve as pseudomorphic III−V/Si(100) quasisubstrates. Single-domain Si(100) surfaces, for example, are a prerequisite for antiphase domain-free III−V heteroepitaxy.[1] Si(100) surface preparation has been studied in great detail: When prepared in H_2 ambient, monohydride-terminated Si dimers form at the Si(100) surface.[2] Their orientation corresponds to the step structure at the surface: The dimer orientation with respect to the step edges is changing from parallel (B-type, (2×1)) to perpendicular (A-type, (1×2)) at adjacent terraces separated by steps of odd numbered atomic heights.[3] A preference for energetically unfavorable[4] A-type Si(100) with 2° misorientation toward [011], however, could be explained by kinetics: The anisotropic diffusion of Si vacancies preferably along dimer rows and their annihilation at the step edges creates A-type terraces.[5] Temperatures of about 750 °C and high H_2 pressures are essential here.[5] Identical conditions applied to almost exactly oriented Si(100) with larger terraces, in contrast, causes layer-by-layer Si removal,[6] which needs to be avoided in order to prepare smooth, single-domain A-type surfaces. We recently studied GaP nucleation on Si(100) and suggested a kinetically limited formation of abrupt heterointerfaces with either Si−P or Si−Ga bonds depending on the (Ga,P) chemical potential during nucleation.[7] For GaP grown on Si(100) in P-rich conditions, we could directly evidence the existence of Si−P bonds with X-ray photoelectron spectroscopy (XPS).[8] Though III−V residuals are inherently present in a realistic processing ambient, Si(100) studies were mainly performed in clean metalorganic vapor phase epitaxy (MOVPE) reactor conditions. The impact of reactor residuals on the formation of the heterointerface is still unclear.

Here, we will discuss the crucial influence of surface misorientation and submonolayer coverages of (Ga,P) residuals on the Si(100) preparation and subsequent GaP nucleation in MOVPE ambient (Aixtron AIX-200). We apply reflection anisotropy spectroscopy (RAS, LayTec EpiRAS-200) throughout processing and benchmark these optical in situ signals to in situ mass spectrometry (MS, Hiden HAL301) as well as low-energy electron diffraction (LEED, Specs ErLEED 100-A) and XPS (Specs Focus 500 and Phoibos 100) accessible after contamination-free sample transfer.[9] RAS measures here the difference in complex reflection along [011] and [0$\bar{1}$1] and is particularly sensitive to (100) surfaces of cubic crystals.[10] Throughout the discussion, we will focus on Si(100) with 0.1° ± 0.05° misorientation toward [011]. Important differences compared to higher misorientations will be discussed. We varied reactor preconditioning and Si preparation to control the amount of (Ga,P) residuals at the Si(100) surface: (1) Samples prepared in a GaP reactor, which was baked at least 30 min at 1010 °C in H_2 and eventually coated with Si, are marked with the index 'clean' and (2) samples prepared in the presence of intentionally higher amounts of residual (Ga,P) species (e.g., by reducing the bakeout time and applying quicker pressure ramps after Si homoepitaxy) are indexed with 'cont'. Identical process

Received: March 13, 2015
Accepted: April 20, 2015
Published: April 20, 2015

DOI: 10.1021/acsami.5b02231
ACS Appl. Mater. Interfaces 2015, 7, 9323−9327

parameters were applied for thermal deoxidation and Si homoepitaxy with silane (SiH_4).[2] In case of GaP/Si samples, subsequent tertbutylphosphine (TBP) and triethylgallium (TEGa) pulses were offered at 420 °C prior to pseudomorphic growth of about 40 nm GaP.[7]

The "P-rich" (2×2)/c(4×2) surface reconstruction of GaP(100) is formed by buckled P dimers, which are stabilized by one H atom each.[11,12] Its LEED patterns consist of spots at half-order (from the (2×1)-like P dimers) and streaks, both in parallel to the P dimer axis. Due to the zincblende crystal structure, the antiphase domain content at GaP/Si(100) surfaces is reflected in domains of mutually perpendicular P dimers.[13] Figure 1 shows LEED patterns of (2×2)/c(4×2) reconstructed GaP/Si_{clean}. At about the center of the sample, the GaP/Si(100) surface is almost single-domain B-type as indicated by spots at half order along [0$\bar{1}$1] in Figure 1b. These LEED patterns do not change significantly over large areas of the sample. Toward the front edge, however, the spots at half order along [011] increase in intensity (cf. Figure 1c) and at the very edge, the A-type domain even prevails (cf. Figure 1d). Similar behavior is observed at the top and bottom edges. At the rear, in contrast, the B-type majority domains persist (cf. Figure 1a). These findings clearly point to an effect at edges close to the susceptor. Two possible explanations are that (i) already the corresponding domain ratio at the Si(100) surface is affected analogously, or (ii) that diffusion of residual atoms influences the chemical ambient during GaP nucleation.

Figure 2 demonstrates that outgassing of both Ga and P species from reactor parts needs to be considered: After a typcial GaP/Si growth run, we heated the reactor to 1010 °C (950 mbar H_2) and monitored the mass:charge ratios, which relate to P and Ga, with a mass spectrometer connected to the reactor outlet. While we cannot directly translate the measured ionization currents to partial pressures in the reactor, both Ga, GaH_x, P and PH_x species are clearly present in the gas phase.

In order to study the effect of background residuals quantitatively, we performed XPS measurements. Coverages were quantitatively estimated applying a model described in ref 14 including the Si 2p plasmon loss peak. One ML would correspond to the thickness of a quarter of a lattice constant with every atomic substrate site replaced by the overlayer

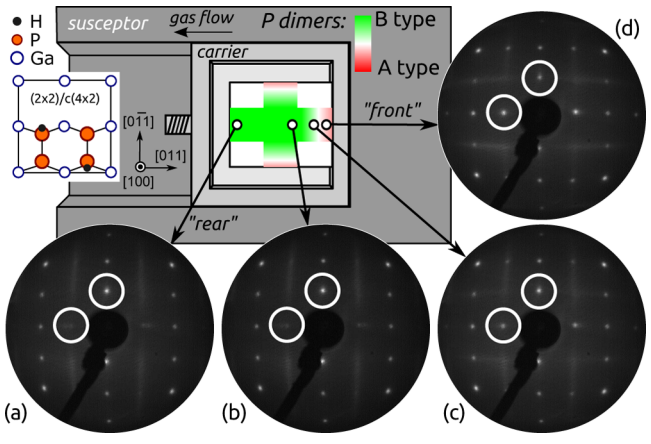

Figure 1. (a–d) LEED patterns (E = 102 eV) of (2×2)/c(4×2) reconstructed GaP/Si_{clean} and qualitative sketch of the sample (length ≈ 2 cm) with color-coded domain imbalance along a scan parallel and perpendicular to the flow direction. The inset (left) shows a top view on the (2×2)/c(4×2) surface reconstruction.

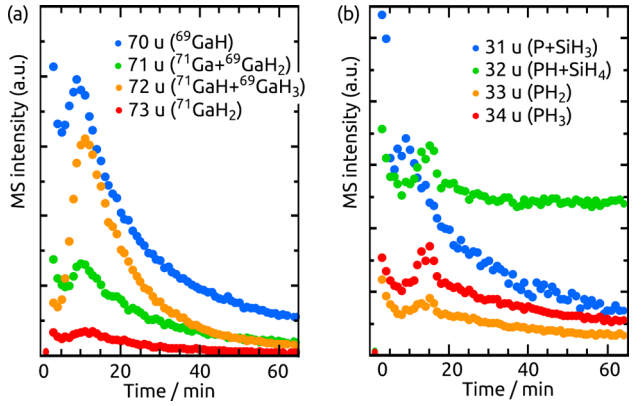

Figure 2. Mass spectrometry during heating (no sample, 950 mbar H_2, 1010 °C reached at 16 min) after a GaP/Si(100) process. (a) Ga-related species, (b) P-related species.

species. Here, we compare Si_{clean} to Si_{cont}, where we increased the reactor pressure gradient after Si buffer growth. Both samples were transferred to XPS[9] after Si(100) processing and prior to pulsed GaP nucleation. Figure 3 shows selected PE lines and Table 1 gives binding energies (E_B) and coverages. For both samples, the Ga $2p_{3/2}$ photoemission (PE) line (Figure 3a) clearly consists of two components: a bigger component (Ga_2) and a smaller one at lower binding energies (Ga_1). Compared to recently published data for a thicker GaP/Si(100) reference,[8] the entire spectrum is shifted toward higher binding energies as the Fermi level at the surface here is located closer to the conduction band. Considering that shift, Ga_2 matches the position of GaP. Due to the small cross-section and lower surface-sensitivity, the P 2p PE line (Figure 3b) of Si_{cont} is not intense enough to reliably distinguish between the existence of two or just one component. The different ratio of Ga_2:P between the samples could explain the shift of the P 2p line position, as the two chemically shifted components, one would expect, cannot be reliably resolved. Si_{cont}, however, is covered by about 9 times more Ga and about 2 times more P compared to Si_{clean}. Intensity ratios were calculated using SPECS ASF factors assuming a homogeneous element distribution. For thin layers, this underrates PE lines at higher kinetic energies, which explains the different ratio when compared to the ML coverage. When Si_{cont} is measured at 30° exit angle to raise surface sensitivity, the ratio Ga_1:Ga_2 increases, whereas Ga_1:P remains constant (see Table 1). This implies that the Ga_2 signal is more attenuated than that of Ga_1 and P. We interpret this as Ga_2 being covered by another species, while Ga_1 and P are not. One possible explanation is that three different adsorbate species coexist at the surface: (i) about 9% of a monolayer (ML) GaP, where Ga (the Ga_2 component) is situated below P, (ii) about 8% ML of P-species not bound to Ga, and (iii) about 1% ML Ga-species (the Ga_1 component) not bound to P. The Si 2p PE line (Figure 3c) cannot sufficiently be fitted by neither one single component, nor by two components, because of the low coverages. Consequently, the Si 2p PE line does not allow a clear conclusion on whether the Ga and the P species are chemically bound to Si. Position-dependent measurements at 90° exit angle of Si_{cont} suggest a decreasing Ga:P ratio in flow direction (rear, Ga_1:P = 0.14, Ga_2:P = 0.36; front, Ga_1:P = 0.17, Ga_2:P = 0.74) with higher amounts of Ga at the front and more P at the rear of the sample.

DOI: 10.1021/acsami.5b02231
ACS Appl. Mater. Interfaces 2015, 7, 9323–9327

Table 1. Quantification of the $2p_{3/2}$ PE components measured by XPS (cf. Figure 3)[a]

	Si_{clean}		Si_{cont}				
PE line	E_B (eV)	C/ML (%)	E_B (eV)	C/ML (%)	ratio	90°	30°
Ga_1	1116.53	0.4	1116.28	1.3	Ga_1:Ga_2	0.17	0.39
Ga_2	1117.58	0.7	1117.48	8.6	Ga_1:P	0.10	0.11
P	129.38	8	129.09	17	Ga_2:P	0.68	0.28
Si	99.76		99.65				

[a]Coverages C are given in % ML according to ref 14. E_B is given with respect to E_F. Intensity ratios were corrected with atomic sensitivity factors (ASF).

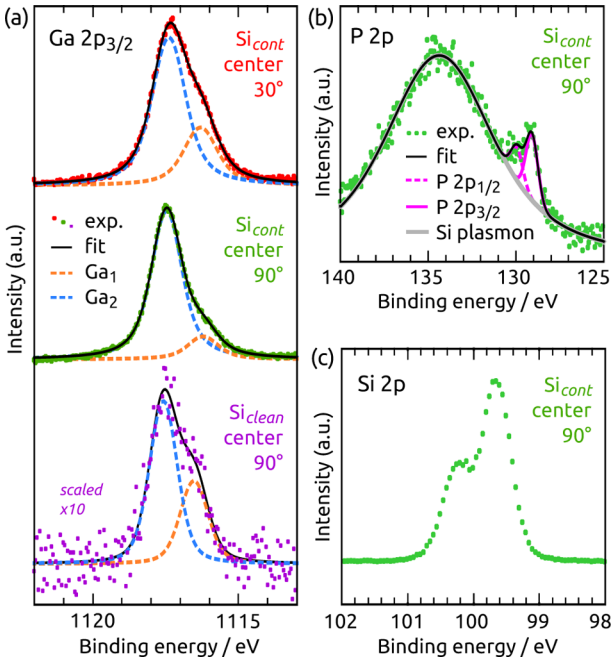

Figure 3. XPS measurements (monochromated Al K_α). (a) Ga $2p_{3/2}$ PE line and fit components of Si_{cont} measured at normal photoelectron exit angle (green) and 30° exit angle (red) as well as of Si_{clean} (violet). (b) P 2p PE line of Si_{cont} measured at normal exit angle and fit components including the Si 2p plasmon loss peak at 134.37 eV (fwhm = 7.4 eV). (c) Si 2p PE line of Si_{cont} measured at normal exit angle. Binding energies are given with reference to the Fermi level.

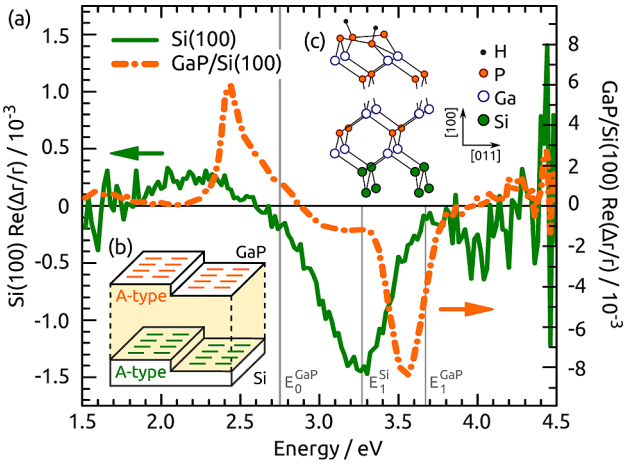

Figure 4. (a) RA spectra of Si_{cont} directly prior to GaP nucleation (420 °C) and of subsequently grown, (2×2)/c(4×2) reconstructed GaP (50 °C). (b) Corresponding orientations of P and Si dimers (prior to nucleation). (c) Sketch of the heterointerface in the abrupt model. Vertical gray lines indicate the critical point energies of Si[18] and GaP,[19] respectively.

Figure 4 shows the RA spectra of one single Si_{cont} sample directly prior to nucleation as well as of (2×2)/c(4×2) reconstructed GaP/Si_{cont} after heteroepitaxy. The Si(100) signal (green, solid line) is similar to that of H-terminated Si(100), though there are slight differences: Beyond 3.9 eV, RAS of Si_{cont} does not clearly show the peaklike contribution known from clean H-terminated Si(100),[5,15] but an additional broad peak seems present around 2.2 eV. The clear peak at the E_1 interband transition of Si, however, corresponds to a preferential A-type Si dimer orientation, which is indicated in the inset b. RA spectra of (2×2)/c(4×2) reconstructed GaP/Si(100) are related to the buckled P dimers and the sign of the RAS signal (at the surface-modified bulk transition below E_1 of GaP and at the transition at about 2.5 eV) corresponds to the P dimer orientation.[11−13,16] The GaP/Si_{cont} RA spectrum measured here (orange, dash-dotted line) corresponds to majority A-type P dimers. The intensity, however, indicates that antiphase disorder did not completely annihilate.[13] Hence, in this case, RAS proves growth of majority A-type GaP on preferential A-type Si. Within an abrupt interface model,[7,17] the case A → A implies Si−Ga bonds at the heterointerface as indicated in the inset c of Figure 4.

Both for GaP growth on Si_{clean} (see Figure 1a) and Si(100) with 2° offcut,[7] in contrast, the GaP sublattice orientation is inverted, which implies Si−P bonds at the heterointerface.[7] In principle, the inversion of the GaP sublattice could also be explained by Si−P bonds combined with either (i) B-type Si(100), (ii) substitutional P adsorption or (iii) an additional Ga/P interlayer forming one ML below the uppermost Si atoms. However, these processes would then only occur during pulsed nucleation on Si_{cont} and not on Si_{clean}. Note that our experiments differ from As-terminated Ge(100).[20,21] Here, we vary the amount of sub-ML residuals on Si with A-type majority domains. Subsequently, pulsed nucleation with precursor supply is performed identically. We observed Si−P bonds and a GaP sublattice orientation in disagreement with substitutional P adsorption of a whole Si ML in ref 8 during GaP nucleation in comparably clean systems. In case of Si_{cont}, our XPS analysis indicates that P is adsorbed on top of Si. Consequently, it seems unlikely that P will substitute Si atoms during subsequent GaP nucleation. Ga was found to promote B-type Si(100) terraces at Si(100), which was Joule-heated to 600 °C in UHV.[22] To explain our findings, rearrangement toward Ga-covered B-type Si terraces[22] would have to take place during pulsed nucleation simultaneously with replacement of the uppermost Ga atoms by P, which we find unlikely. Ga droplet growth on Si(100) terraces with precursor supply may lead to pyramidal etching.[23,24] The droplet formation was found to be significantly above 1 ML of Ga and can be reduced by higher

DOI: 10.1021/acsami.5b02231
ACS Appl. Mater. Interfaces 2015, 7, 9323−9327

V:III ratios.[25] Here, Ga coverages prior to nucleation are clearly below 1 ML and XPS results even imply that the larger Ga_2 component, which is not located at the very surface, is bound to P, whereas the Ga_1 component is on top. Regarding Ga coverages below 0.5 ML, UHV studies suggest that Ga−Ga dimers form on top of Si dimers, which remain unbroken.[26−28] Though experimental conditions are quite different here (monohydride terminated Si, presence of P), intact A-type Si dimers below the adsorbed Ga could explain the Si dimer related RAS minimum at E_1^{Si} (Figure 4) and possibly also the slight differences in line shape above and below E_1^{Si} compared to Si(100) prepared in absence of III−V residuals.[5] The increased amount of Ga available during GaP nucleation also shifts the (P,Ga) chemical potential toward more Ga-rich conditions. Ab initio density functional theory calculations showed that the energetically favorable binding situation at abrupt GaP/Si(100) heterointerfaces changes from Si−P to Si−Ga for more Ga-rich nucleation conditions,[7] which can explain the observation of inverted GaP sublattice growth on Si_{clean} and Si_{cont}. It may also explain the Si−Ga bonds suggested recently.[17]

We believe that the Si surface preparation step after Si buffer growth is decisive here for the amount of residuals found on the surface. Annealing at 730 °C in 950 mbar H_2 after thermal deoxidation at 1000 °C is crucial for single-domain, A-type surface preparation of Si(100) 2°.[5] Quick temperature and pressure ramps, however, are necessary to avoid layer-by-layer removal on Si(100) 0.1° occurring in this temperature range.[6] Particularly the pressure ramp is complicating Si(100) 0.1° surface preparation in reactors contaminated with III−V residuals: The rate of residuals desorbing from reactor parts (liner, susceptor, carrier) is increasing with decreasing pressure. This becomes particularly important at elevated temperatures, where desorption of residuals from reactor parts and diffusion of residuals on the sample are high, whereas the H termination[2] is not stable yet. The consequence is that single-domain surface formation and avoidance of contamination conflict for nominal Si(100) substrates regarding process parameters. The residual atoms may also influence Si vacancy generation and diffusion, but in situ RAS reveals an A-type majority domains even for Si_{cont} so that we believe that the kinetic surface processes are comparable to ref.[6] Nucleation with a starting TEGa pulse (not shown here) was not sufficient to grow GaP with majority A-type P dimers. Nucleation with high residual amounts or high TEGa precursor supply−in order to reach high amounts of Ga for single-domain GaP−is not easy to control. The coexistence of areas with Si−P and Si−Ga bonds at single-domain Si(100) terraces, however, would cause antiphase disorder analogously to the existence of either Si−P or Si−Ga bonds at two-domain Si(100) terraces. We never observed A-type GaP/Si(100) surfaces in case of A-type Si(100) 2° misoriented substrates. Cooling to temperatures below 730 °C in 950 mbar H_2 (for annealing to prepare A-type terraces) prior to decreasing the reactor pressure for GaP nucleation seems to effectively hinder excessive Ga diffusion on the surface. Both decreased desorption rates from reactor parts and the H termination of the Si(100) surface[2] are benificial here. Nucleation on nominally oriented Si(100) may also benefit from even higher TBP partial pressures.

In conclusion, we showed that a compromise between the avoidance of layer-by-layer removal and diffusion of (Ga,P) residuals to the substrate must be made for Si(100) surface preparation. Submonolayer coverages of (Ga,P) residuals on the Si(100) surface−prior to offering precursors for pulsed nucleation−strongly influence GaP nucleation. The majority GaP sublattice orientation changes for higher amounts of Ga present at the surface. We explain this by a dependency of abrupt heterointerface structures on the chemical potential during nucleation[7] and the presence of Si−Ga nucleation seeds prior to offering the first precursor pulse. The coexistence of Si−P and Si−Ga bond domains can lead to antiphase disorder in the GaP epilayer. Consequently, the residual background pressure needs to be controlled precisely for well-defined interface preparation. Time-resolved studies are planned in order to resolve the optical anisotropy of the presumably Si−Ga heterointerfaces.

AUTHOR INFORMATION

Corresponding Author

*E-mail: oliver.supplie@tu-ilmenau.de.

Notes

The authors declare no competing financial interest.

ACKNOWLEDGMENTS

It is a pleasure to thank W. Daum, G. Lilienkamp, B. Borkenhagen, F. Grosse, and O. Romanyuk for valuable discussions. This work was financially supported by the DFG (proj. no. HA3096/4-1).

REFERENCES

(1) Kroemer, H. Polar-on-Nonpolar Epitaxy. *J. Cryst. Growth* **1987**, *81*, 193−204.

(2) Brückner, S.; Döscher, H.; Kleinschmidt, P.; Hannappel, T. In Situ Investigation of Hydrogen Interacting with Si(100). *Appl. Phys. Lett.* **2011**, *98*, 211909.

(3) Chadi, D. J. Stabilities of Single-Layer and Bilayer Steps on Si(001) Surfaces. *Phys. Rev. Lett.* **1987**, *59*, 1691−1694.

(4) Laracuente, A. R.; Whitman, L. J. Step Structure and Surface Morphology of Hydrogen-Terminated Silicon: (001) to (114). *Surf. Sci.* **2003**, *545*, 70−84.

(5) Brückner, S.; Döscher, H.; Kleinschmidt, P.; Supplie, O.; Dobrich, A.; Hannappel, T. Anomalous Double-Layer Step Formation on Si(100) in Hydrogen Process Ambient. *Phys. Rev. B* **2012**, *86*, 195310.

(6) Brückner, S.; Kleinschmidt, P.; Supplie, O.; Döscher, H.; Hannappel, T. Domain-Sensitive In Situ Observation of Layer-by-Layer Removal at Si(100) in H_2 Ambient. *New J. Phys.* **2013**, *15*, 113049.

(7) Supplie, O.; Brückner, S.; Romanyuk, O.; Döscher, H.; Höhn, C.; May, M. M.; Kleinschmidt, P.; Grosse, F.; Hannappel, T. Atomic Scale Analysis of the GaP/Si(100) Heterointerface by in situ Reflection Anisotropy Spectroscopy and *ab initio* Density Functional Theory. *Phys. Rev. B* **2014**, *90*, 235301.

(8) Supplie, O.; May, M. M.; Steinbach, G.; Romanyuk, O.; Grosse, F.; Nägelein, A.; Kleinschmidt, P.; Brückner, S.; Hannappel, T. Time-Resolved Optical In Situ Spectroscopy During Formation of the GaP/Si(100) Heterointerface. *J. Phys. Chem. Lett.* **2015**, *6*, 464.

(9) Hannappel, T.; Visbeck, S.; Töben, L.; Willig, F. Apparatus for Investigating Metalorganic Chemical Vapor Deposition-Grown Semiconductors with Ultrahigh-Vacuum based Techniques. *Rev. Sci. Instrum.* **2004**, *75*, 1297−1304.

(10) Aspnes, D. E.; Studna, A. A. Anisotropies in the Above-Band-Gap Optical Spectra of Cubic Semiconductors. *Phys. Rev. Lett.* **1985**, *54*, 1956−1959.

(11) Töben, L.; Hannappel, T.; Möller, K.; Crawack, H.; Pettenkofer, C.; Willig, F. RDS, LEED and STM of the P-rich and Ga-rich Surfaces of GaP(100). *Surf. Sci.* **2001**, *494*, L755−L760.

(12) Hahn, P. H.; Schmidt, W. G.; Bechstedt, F.; Pulci, O.; Sole, R. D. P-rich GaP(001)(2 × 1)/(2 × 2) Surface: A Hydrogen-Adsorbate

DOI: 10.1021/acsami.5b02231
ACS Appl. Mater. Interfaces 2015, 7, 9323−9327

Structure Determined from First-Principles Calculations. *Phys. Rev. B* **2003**, *68*, 033311.
(13) Döscher, H.; Hannappel, T. In Situ Reflection Anisotropy Spectroscopy Analysis of Heteroepitaxial GaP Films Grown on Si(100). *J. Appl. Phys.* **2010**, *107*, 123523.
(14) May, M.; Lewerenz, H.-J.; Hannappel, T. Optical In Situ Study of InP(100) Surface Chemistry: Dissociative Adsorption of Water and Oxygen. *J. Phys.Chem. C* **2014**, *118*, 19032−19041.
(15) Palummo, M.; Witkowski, N.; Pluchery, O.; Del Sole, R.; Borensztein, Y. Reflectance-Anisotropy Spectroscopy and Surface Differential Reflectance Spectra at the Si(100) Surface: Combined Experimental and Theoretical Study. *Phys. Rev. B* **2009**, *79*, 035327.
(16) Sippel, P.; Supplie, O.; May, M. M.; Eichberger, R.; Hannappel, T. Electronic Structures of GaP(100) Surface Reconstructions Probed with Two-Photon Photoemission Spectroscopy. *Phys. Rev. B* **2014**, *89*, 165312.
(17) Beyer, A.; Ohlmann, J.; Liebich, S.; Heim, H.; Witte, G.; Stolz, W.; Volz, K. GaP Heteroepitaxy on Si(001): Correlation of Si-Surface Structure, GaP Growth Conditions, and Si-III/V Interface Structure. *J. Appl. Phys.* **2012**, *111*, 083534.
(18) Lautenschlager, P.; Garriga, M.; Vina, L.; Cardona, M. Temperature Dependence of the Dielectric Function and Interband Critical Points in Silicon. *Phys. Rev. B* **1987**, *36*, 4821.
(19) Zollner, S.; Garriga, M.; Kircher, J.; Humlícek, J.; Cardona, M.; Neuhold, G. Temperature Dependence of the Dielectric Function and the Interband Critical-Point Parameters of GaP. *Thin Solid Films* **1993**, *233*, 185−188.
(20) Brückner, S.; Supplie, O.; Barrigón, E.; Luczak, J.; Kleinschmidt, P.; Rey-Stolle, I.; Döscher, H.; Hannappel, T. In Situ Control of As Dimer Orientation on Ge(100) Surfaces. *Appl. Phys. Lett.* **2012**, *101*, 121602.
(21) Ting, S. M.; Fitzgerald, E. A. Metal-Organic Chemical Vapor Deposition of Single Domain GaAs on Ge/Ge_xSi_{1x}/Si and Ge Substrates. *J. Appl. Phys.* **2000**, *87*, 2618−2628.
(22) Hara, S.; Irokawa, K.; Miki, H.; Kawazu, A.; Torii, H.; Fujishiro, H. I. Behavior of Ga atoms on Si(001) Surface at High Temperature. *J. Appl. Phys.* **2005**, *98*, 083513−0835137.
(23) Bell, K. A.; Ebert, M.; Yoo, S. D.; Flock, K.; Aspnes, D. E. Real-Time Optical Characterization of Heteroepitaxy by Organometallic Chemical Vapor Deposition. *J. Vac. Sci. Technol. A* **2000**, *18*, 1184−1189.
(24) Werner, K.; Beyer, A.; Oelerich, J.; Baranovskii, S.; Stolz, W.; Volz, K. Structural Characteristics of Gallium Metal Deposited on Si(001) by MOCVD. *J. Cryst. Growth* **2014**, *405*, 102−109.
(25) Volz, K.; Beyer, A.; Witte, W.; Ohlmann, J.; Németh, I.; Kunert, B.; Stolz, W. GaP-Nucleation on Exact Si(001) Substrates for III/V Device Integration. *J. Cryst. Growth* **2011**, *315*, 37−47.
(26) Bourguignon, B.; Carleton, K. L.; Leone, S. R. Surface Structures and Growth Mechanism of Ga on Si(100) Determined by LEED and Auger Electron Spectroscopy. *Surf. Sci.* **1988**, *204*, 455−472.
(27) Baski, A. A.; Nogami, J.; Quate, C. F. Gallium Growth and Reconstruction on the Si(100) Surface. *J. Vac. Sci. Technol. A* **1990**, *8*, 245−248.
(28) Sakama, H.; Kawazu, A.; Sueyoshi, T.; Sato, T.; Iwatsuki, M. Scanning Tunneling Microscopy on Ga/Si(100). *Phys. Rev. B* **1996**, *54*, 8756−8760.

DOI: 10.1021/acsami.5b02231
ACS Appl. Mater. Interfaces 2015, 7, 9323−9327